Periodic Motion Control of the Reaction Wheel Pendulum

Christoph Gruber
and Michael Hofbaur
Institute of Automation
and Control Engineering
UMIT
6060 Hall in Tyrol, Austria
Email: christoph.gruber@umit.at
michael.hofbaur@umit.at

***Abstract*— The reaction wheel pendulum is a mechanism consisting of a planar freely rotating rotating bar with an actuated reaction wheel at its tip. Acceleration of the reaction wheel provides the momentum to swing the pendulum. We apply a modern method from nonlinear control for shaping periodic motions and designing a dedicated stabilizing controller. Specific periodic motions are planned by introducing virtual holonomic constraints and design of a stabilizing controller based on a thorough analysis of the dynamics transversal to the resulting limit cycle. Compared to previous applications, we focus on a concise formulation of the control law and minimize the resulting design and implementation effort.**

I. Introduction

The Reaction Wheel Pendulum (RWP) or also known as inertia wheel pendulum is a typical setup for education and demonstration in the field of nonlinear control systems. It is an introducing example for design and implementation of local linearization-based state feedback controllers to locally stabilize equilibria. More advanced controllers also allow to switch between equilibria. Because of its interesting model properties, many different approaches were evaluated on the RWP.

An energy-based swing-up controller which is able to swing the pendulum up even with saturated control input was developed in [1], [2]. For stabilizing the upward equilibrium they compared the afore-mentioned state feedback controller to a partial feedback linearization design. Another approach that uses switching between multiple controllers was presented by [3], who use qualitative methods to design a controller that robustly stabilizes the upright equilibrium. The same problem was solved by [4], [5] with a single output feedback controller, which was designed using a passivity based method.

Another interesting and challenging task with the RWP is the stabilization of periodic motions. A two-relays controller which was parametrized by analysis of the closed-loop dynamics using the describing function method was presented in [6]. Another approach for stabilizing periodic motions around the upper equilibrium of the RWP was presented in [7]. There, a method developed in [8], [9], [10] was applied for planning periodic motions and designing of a stabilizing controller. This procedure follows three steps: 1) motion planning using virtual constraints; 2) computing a partial feedback transformation; 3) design of a feedback controller to stabilize the origin of a reduced-order linear system with periodic coefficients, which corresponds to a linearization of the dynamics transversal to the periodic motion. For the latter step, [7], [8], [9], [10], proposed the design of a Linear Quadratic Regulator (LQR).

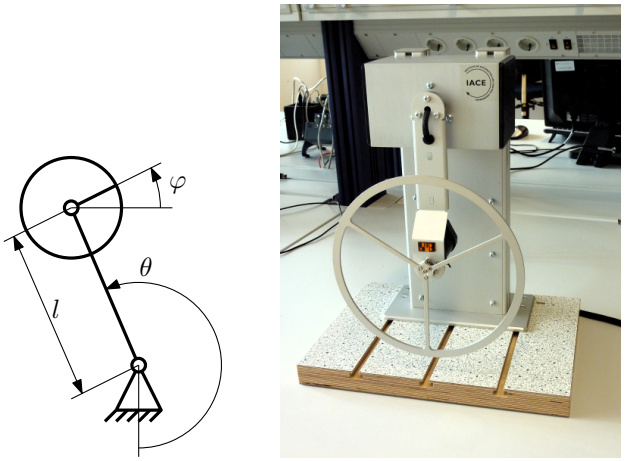

Fig. 1. Left: Sketch of the reaction wheel pendulum. Right: experimental hardware.

In this paper, we apply the method from [8], [9], [10]. However, a simpler approach to design a controller for stabilization of the origin of the linearized transverse dynamics is used. Thereby, we present a simple-as-possible application of the method, such that the results can be reproduced easily.

The remainder of this paper is organized as follows: Sec. II presents the hardware of our (commercially available) experimental setup. Furthermore, a model is built and its main properties are introduced briefly. The model is given in several different representations, since all these will be referenced in later sections. The issue of motion planning is tackled in Sec. III. There, we mainly use results from [9] to choose a periodic motion which is consistent with the dynamics of the RWP. Sec. IV is subdivided into 3 parts: IV-A follows the step-by-step procedure from [8] to reduce the nonlinear RWP dynamics to a

TABLE I

MODEL PARAMETERS

Symbol	Value [Unit]	Meaning
J	0.0135 [kg m^2]	inertia of the pendulum assembly
J_a	0.0012 [kg m^2]	inertia of the reaction wheel
m	0.416 [kg]	mass of the pendulum assembly
g	9.81 [ms^{-2}]	gravity constant
l	0.175 [m]	length of the pendulum bar
r	3.71 [1]	gearbox transmission ratio
η_g	0.79 [1]	gearbox efficiency
η_d	0.8 [1]	DC-Motor efficiency
k	0.0346 [NmA^{-1}]	DC-Motor torque constant
R_a	5.78 [Ω]	DC-Motor armature resistance

linear system with periodic coefficients. Our main contribution is presented in Sec. IV-B, which is a state feedback controller that is simple to design and simple to implement. Finally, to conclude control design, Sec. IV-C shows the design of a high gain observer to estimate angular rates from encoder measurements. Sec. V compares a LQR with our controller by simulations. Experimental results are presented in Sec. VI and Sec. VII concludes the paper.

II. HARDWARE AND MODELING

The reaction wheel pendulum hardware used in this research is a commercially available platform from B&R Automation shown in Fig. 1. The equations of motion are easily found by using the formalism of Lagrange. Simplifying, we assume a two-mass model where masses are concentrated in the centers of mass of the corresponding bodies. The mass m of the pendulum assembly consists of the bar, the bolt of the pendulum bearing, electric drive, gearbox, cables and the reaction wheel. The principal inertia of the bar assembly about the axis of the pendulum bearing is J. The principal inertia of the reaction wheel is J_a. Furthermore, we assume all bodies to be perfectly rigid and consider all motions to evolve in a plane perpendicular to the axis of the pendulum bearing. Thus, the configuration manifold M of the resulting model is the 2-torus $\mathbb{T}^2$. Model parameters are summarized in Tab. I. Using the angle θ between the bar and the vertical axis and the angle φ of the reaction wheel relative to the horizontal line (see Fig. 1) as generalized coordinates gives the equations of motion:

$$\begin{aligned} mgl\sin(\theta) + J\ddot{\theta} + J_a\ddot{\varphi} &= 0 \\ J_a\ddot{\varphi} &= \tau_M \end{aligned} \tag{1}$$

where τ_M is the torque applied by a (permanent magnet brushed) dc-motor over a planetary gear. The motor is modeled as

$$\tau_M = \frac{rk\eta_d\eta_g}{R_a}\left(v - kr(\dot{\varphi} - \dot{\theta})\right) \tag{2}$$

with v the motor voltage. We assume that the electrical is much faster than the mechanical dynamics. Thus, we neglect the armature inductance. The equations of motion can equivalently be rewritten in matrix form:

$$M\ \ddot{q} + C\ \dot{q} + G(q) = B\ v \tag{3}$$

with

$$M = \begin{bmatrix} J_aR_a & 0 \\ J_a & J \end{bmatrix}, \quad C = \begin{bmatrix} k^2r^2\eta_d\eta_g & k^2r^2\eta_d\eta_g \\ 0 & 0 \end{bmatrix},$$

$$G(q) = \begin{bmatrix} 0 \\ mgl\sin(\theta) \end{bmatrix}, \quad B = \begin{bmatrix} kr\eta_d\eta_g \\ 0 \end{bmatrix}, \quad q = \begin{bmatrix} \varphi \\ \theta \end{bmatrix}.$$

or in state-space representation:

$$\dot{x} = f(x, v) \tag{4}$$

$$= \begin{bmatrix} x_3 \\ x_4 \\ -\frac{mgl\sin(x_1)}{J} - \frac{kr\eta_d\eta_g(v - krx_4 + krx_3)}{R_aJ} \\ \frac{kr\eta_d\eta_g(v - krx_4 + krx_3)}{R_aJ_a} \end{bmatrix} \tag{5}$$

with $x = [\theta\ \varphi\ \dot{\theta}\ \dot{\varphi}]^T$. Since there are two degrees of freedom (DoFs) but only one actuator, the reaction wheel pendulum is an underactuated system with underactuation degree one. The angles θ and φ are measured using encoders with a resolution of 4096 [cnt/rev] and $r \cdot 2000$ [cnt/rev], respectively[1]. System (4) has four state variables but can be reduced to three $(\theta, \dot{\theta}, \dot{\varphi})$, since $x_2 = \varphi$ does not occur in the other equations. The voltage v is an input and the equilibria of the reduced system are found at $(\theta_E = k\pi,\ \dot{\theta}_E = 0,\ \dot{\varphi}_E = 0),\ k \in \mathbb{Z}$, where equilibria with k odd correspond to the pendulum bar pointing upwards and k even downwards. The upward equilibria are unstable, while the downward are stable, which is easily verified by computing the eigenvalues of the Jacobian at equilibrium. These properties - configuration manifold $\mathbb{T}^2$, underactuation and existence of stable and unstable equilibria - make the reaction wheel pendulum an interesting model for control engineers.

III. MOTION PLANNING

The motions that we want to shape need to respect the dynamics of the reaction wheel pendulum. There exist multiple approaches to solve such a motion planning problem [11]: One way would be to parametrize the desired motion and involve the dynamics as constraint. Another method is employing virtual constraints [12]: Relations between DoF are parametrized and introduced into the dynamics. The parameters of these relations (the virtual constraints) show up in expressions for the resulting motions and can be tuned to arrive at a desired motion. Introducing a rather general virtual constraint in the form

$$\varphi = f(\theta) = F(\theta) + \varphi_0 \tag{6}$$

with constant φ_0 and $F(\theta) \in \mathcal{C}^2(\mathbb{S}^1)$ allows the reduction of the model (1) to a single differential equation

$$mgl\sin(\theta) + J\ddot{\theta} + J_a\frac{\mathrm{d}^2}{\mathrm{d}t^2}(F(\theta) + \varphi_0) = 0 \tag{7}$$

which represents the dynamics of the RWP when the virtual constraint (6) is perfectly met. The solutions of this ordinary differential equation are motions that are consistent with the dynamics of the RWP and the virtual constraint. Thus, by

[1]The encoder for φ is mounted at motor side

choosing specific $F(\theta)$ and φ_0 motions can be designed. φ_0 can be understood as an angular offset between θ and φ. Since the goal was to design a periodic motion, further conditions need to be incorporated such that the resulting motion is a limit cycle. Consequently, we proceed according to the method presented in [9]: Collecting the appropriate terms leads to the so-called homogeneous $\alpha\beta\gamma$ equation:

$$\alpha(\theta)\ddot{\theta} + \beta(\theta)\dot{\theta}^2 + \gamma(\theta) = 0 \tag{8}$$

with

$$\begin{aligned} \alpha(\theta) &= J + J_a \frac{\mathrm{d}F}{\mathrm{d}\theta}, \\ \beta(\theta) &= J_a \frac{\mathrm{d}^2F}{\mathrm{d}\theta^2}, \\ \gamma(\theta) &= mgl\sin(\theta). \end{aligned} \tag{9}$$

The condition [9, Theorem 3] for existence of a limit cycle in (7) around an equilibrium θ_E now reads

$$\begin{aligned} \omega_c^2 &= \left[\frac{\mathrm{d}}{\mathrm{d}\theta}\frac{\gamma(\theta)}{\alpha(\theta)}\right]\Big|_{\theta=\theta_E} \\ &= \frac{-mgl}{(J + J_a \frac{\mathrm{d}F}{\mathrm{d}\theta}(\theta_E))} \\ &> 0 \end{aligned} \tag{10}$$

where $T = \frac{2\pi}{\omega_c}$ is the period of the oscillation.

One possible choice of virtual constraint is

$$\varphi(t) = d_1\theta(t) + \varphi(0). \tag{11}$$

For this specific virtual constraint, the condition for existence of a limit cycle about an upward equilibrium $\theta_E = \pi$ is

$$d_1 < -\frac{J}{J_a}. \tag{12}$$

With constraint (11), $\beta(\theta) = 0$ and the $\alpha\beta\gamma$ equation reduces to the simpler form

$$(J + J_a\ d_1)\ddot{\theta} + mgl\sin(\theta) = 0 \tag{13}$$

which corresponds to the dynamics of the standard physical pendulum. A specific periodic motion $\theta_\star(t+T) = \theta_\star(t)$ is selected by choosing constraint parameters - in our case only d_1 - and initial values $\theta_\star(0)$ and $\dot{\theta}_\star(0)$.

The solutions of (13) are elliptic integrals of the first kind. Quantities $d_1, \theta_\star(0)$ and $\dot{\theta}_\star(0)$ could be chosen such that a desired amplitude is reached, see [7]. However, for more complex virtual constraints such solutions are neither available nor does the presented method require such knowledge. Thus, we will ignore the existence of such a solution in the remainder.

IV. Control Design

Our control design procedure consists of three steps where the first step - a partial feedback linearization - is used to transform the nonlinear control problem to a linear time-varying one [8]. Coordinates of the linear system are coordinates of a section in the tangential bundle TM of M transversal to the limit cycle (a Poincaré section). The second step is the design of a stabilizing controller for the origin of the linear system. In these first two steps the rates $\dot{\theta}$ and $\dot{\varphi}$ are used. For this reason, a high-gain-observer is designed in the third step.

A. Partial Feedback Linearization

In Sec. III we assumed that the virtual constraint is perfectly met. It is the task of a controller to make this virtual constraint invariant. Let us introduce error coordinates

$$\begin{aligned} e(t) &= \varphi(t) - f(\theta(t)) \\ &= \varphi(t) - (d_1\theta(t) + \varphi(0)) \qquad (14) \\ \dot{e}(t) &= \dot{\varphi}(t) - d_1\ \dot{\theta}(t) \qquad (15) \\ \ddot{e}(t) &= \ddot{\varphi}(t) - d_1\ \ddot{\theta}(t). \end{aligned}$$

To compute the partial feedback linearization we follow the step-by-step procedure from [8, Proposition 3]. Our goal is now to write the dynamics of the RWP in coordinates e, $\dot{e}$, $\dot{\theta}$ and θ such that the dynamics of e correspond to a double integrator of a new input ν. Following (14), (15) take

$$L = \begin{bmatrix} 1 & d_1 \\ 0 & 1 \end{bmatrix} \tag{16}$$

such that

$$\dot{q} = L \begin{bmatrix} \dot{e} \\ \dot{\theta} \end{bmatrix} \tag{17}$$

and employ the matrix form of the RWP-dynamics from (3) to find a constant

$$K = \begin{bmatrix} 1 & 0 \end{bmatrix} L^{-1}M^{-1}B. \tag{18}$$

The feedback transformation

$$v = \frac{1}{K}[\nu - R(\theta, \dot{\theta}, \dot{e})] \tag{19}$$

with

$$R(\theta, \dot{\theta}, \dot{e}) = \begin{bmatrix} 1 & 0 \end{bmatrix} L^{-1}M^{-1}(-CL \begin{bmatrix} \dot{e} \\ \dot{\theta} \end{bmatrix} - G(\theta))$$

transforms the Euler-Lagrange system (1) to the partly linear form

$$\begin{aligned} \alpha(\theta)\ddot{\theta} + \beta(\theta)\dot{\theta}^2 + \gamma(\theta) &= u(\nu) \qquad (20) \\ \ddot{e} &= \nu \qquad (21) \end{aligned}$$

where the first equation is the inhomogeneous $\alpha\beta\gamma$ equation with $u(\nu) = -J_a\nu$ and the second one is a double integrator. The resulting (memoryless) feedback transformation is

$$\begin{aligned} v &= \frac{JJ_aR_a\ \nu - J_aR_ad_1mgl\ \sin(\theta)}{kr\eta_d\eta_g(J + J_ad_1)} + \\ &\quad + kr\ \dot{e} + kr(d_1 - 1)\ \dot{\theta}. \end{aligned} \tag{22}$$

To find coordinates for a (Poincaré) section in TM a further coordinate is required. Since the $\alpha\beta\gamma$ equation is integrable, an expression for $\dot{\theta}^2$ can be found. The difference between this expression and the actual $\dot{\theta}^2$ corresponds to a so-called integral of motion I which preserves a zero-value on the limit cycle and can thus be used as third coordinate. This integral of motion is [9, Theorem 1][2]

$$\begin{aligned} I &= \dot{\theta}^2 - \dot{\theta}_\star(0)^2 - \int_{\theta_\star(0)}^{\theta} \frac{-2\gamma(s)}{\alpha(s)}ds \\ &= \dot{\theta}^2 - \dot{\theta}_\star(0)^2 - \frac{2mgl\,(\cos(\theta) - \cos(\theta_\star(0)))}{J + J_ad_1}. \end{aligned} \tag{23}$$

[2]In our case, $k = 0, \beta_1 = 0, \beta_2 = \gamma$.

Furthermore, the time derivative of I evaluated along a solution of (20) is given by [9, Lemma 2]

$$\begin{aligned} \dot{I} &= \frac{2\dot{\theta}}{\alpha(\theta)} u(\nu) \\ &= -\frac{2J_a\dot{\theta}}{J + J_a d_1}\nu =: k_b\dot{\theta}\nu. \end{aligned} \tag{24}$$

The dynamics transversal to the limit cycle can now be written in the compact form (24) and (21). When $\dot{\theta}$ in (21) is the chosen periodic solution $\dot{\theta}_\star$ from Sec. III, then this system reads

$$\dot{x}_\perp = Ax_\perp + b(t)\nu \tag{25}$$

with

$$x_\perp = \begin{bmatrix} I \\ e \\ \dot{e} \end{bmatrix} \quad A = \begin{bmatrix} 0 & 0 & 0 \\ 0 & 0 & 1 \\ 0 & 0 & 0 \end{bmatrix} \quad b(t) = \begin{bmatrix} k_b\dot{\theta}_\star(t) \\ 0 \\ 1 \end{bmatrix}.$$

which is a linear system with periodic coefficients. Note that time-invariance of A is a result of choosing a linear virtual constraint. In general, $A(t)$ would be time-dependent, but (25) would still be a linear system with periodic coefficients with $\dot{\theta}_\star(t)$ being the only function causing time dependence.

B. Regulator Design

Since $A, b(t)$ is controllable over the period [7], it is possible to design a controller that exponentially stabilizes the origin of the Linear Time Varying (LTV) system (25). This is equivalent to finding a stabilizing controller for the origin of the nonlinear transverse dynamics (24), (21) [10, Theorem 2] . For this task, we propose the following state feedback controller[3]:

$$\nu(t, x_\perp) = -\begin{bmatrix} k_1\dot{\theta}(t) & k_2 & k_3 \end{bmatrix} x_\perp. \tag{26}$$

The closed loop system (21), (24), (26) is then given by

$$\dot{x}_\perp = \mathcal{A}(t)x_\perp \tag{27}$$

with

$$\mathcal{A}(t) = \begin{bmatrix} -k_1k_b\dot{\theta}(t)^2 & -k_2k_b\dot{\theta}(t) & -k_3k_b\dot{\theta}(t) \\ 0 & 0 & 1 \\ -k_1\dot{\theta}(t) & -k_2 & -k_3 \end{bmatrix}. \tag{28}$$

We will first show stability of the linearized closed loop system:

Lemma 1: The time-varying state feedback controller from (26) evaluated at $\dot{\theta}_\star$:

$$\nu(t, x_\perp)|_{\dot{\theta}=\dot{\theta}_\star} \tag{29}$$

with k_1, k_2, k_3 such that

$$k_1 \geq \frac{k_2 + k_3}{\sup_{t\in[0,T]} \dot{\theta}_\star(t)} \tag{30}$$

$$k_2, k_3 > 0, \text{ small} \tag{31}$$

locally exponentially stabilizes the origin of the linear system (25).

[3]Note that this is no static gain state feedback controller.

Proof: We will use the averaging method from [13, Chap. 10.4] to show exponential stability of the origin of (27) at $\dot{\theta} = \dot{\theta}_\star$: Take the average system as

$$\dot{\bar{x}}_\perp = \bar{\mathcal{A}}\ \bar{x}_\perp \tag{32}$$

with

$$\begin{aligned} \bar{\mathcal{A}} &= \frac{1}{T}\int_0^T \mathcal{A}|_{\dot{\theta}=\dot{\theta}_\star}(\sigma)d\sigma \\ &= \begin{bmatrix} -k_1k_b\dot{\bar{\theta}}_\star^2 & 0 & 0 \\ 0 & 0 & 1 \\ 0 & -k_2 & -k_3 \end{bmatrix} \end{aligned} \tag{33}$$

where

$$\dot{\bar{\theta}}_\star^2 = \frac{1}{T}\int_0^T \dot{\theta}_\star(\sigma)^2 d\sigma.$$

The zeros in the first and last row of $\bar{\mathcal{A}}$ follow from the integration of a symmetric periodic signal over one period. The condition from (30) is a trade-off between ensuring that the first entry is dominant in the first row of $\mathcal{A}(t)$ and keeping the first entry of the last row small. However, the first entry in the last row can be interpreted as input (or perturbation) to the filter[4] $x_{\perp,2}, x_{\perp,3}$ with low-pass characteristics and coefficients k_2, k_3. Thus, with k_2, k_3 sufficiently small, the cut-off frequency of the filter can be placed low enough to filter $\dot{\theta}$. With $k_1, k_2, k_3 > 0$, $\bar{\mathcal{A}}$ is Hurwitz, since $k_b > 0$ when (12) is satisfied. Take $t = \varepsilon\tau$, ε small and positive, then

$$\frac{\mathrm{d}x_\perp}{\mathrm{d}\tau} = \varepsilon\ \mathcal{A}(\tau)|_{\dot{\theta}=\dot{\theta}_\star}\ x_\perp \tag{34}$$

$$\frac{\mathrm{d}\bar{x}_\perp}{\mathrm{d}\tau} = \varepsilon\ \bar{\mathcal{A}}\ \bar{x}_\perp \tag{35}$$

and, according to [13, Theorem 10.4], the origin of (27) at $\dot{\theta} = \dot{\theta}_\star$ is locally exponentially stable. ■

Note that choosing k_1, k_2 and k_3 is, as usual, a trade-off: Low gains mean slower convergence, but the approximation by the average system will be better and vice versa.

Implementing this controller would require $\dot{\theta}_\star$ to be generated or obtained from a look-up-table. However, $\dot{\theta}$ is available anyway as an estimate from our observer. If we were able to show that the controller from (26) is able to stabilize the origin of the nonlinear system (21), (24), then implementation of this controller would be as simple as implementing a static gain state feedback controller.

Theorem 1: The state feedback controller from (26) orbitally exponentially stabilizes the periodic solution $\theta_\star$ of (20), (21), (26) if the controller is parametrized as in Lemma 1.

Proof: We begin this proof with a property that will be useful in the remaining part of the proof:

Property 1: The closed loop system (20), (21), (22), (26) is a smooth nonlinear system and the target periodic motion $\theta_\star$ a smooth solution. This solution depends continuously on

[4]which already is in controllability canonical form

the initial conditions. This means that it is possible to choose initial values

$$w_1(0) = \begin{bmatrix} \theta_1 & \dot{\theta}_1 & e_1 & \dot{e}_1 \end{bmatrix}^T$$

in $\delta_\star(\varepsilon_\star)$-distance to the limit cycle such that

$$||w_1(t) - w_0(t)|| < \varepsilon_\star, \ t \in [0, T] \tag{36}$$

where $w_0(t)$ is on the orbit $\forall t$ and $\varepsilon_\star$ a positive constant. This holds irrespective of stability of the orbit and only on the finite time interval.

By taking a closer look at the proof of [13, Theorem 10.4], the ultimate condition for the average system (32) to be an $\mathcal{O}(\varepsilon)$ approximation of the closed-loop system (27) is that the origin of the average system must be exponentially stable and with

$$\begin{aligned} \mathcal{A}_\Delta(t) &= \left[\mathcal{A}(t) - \bar{\mathcal{A}}\right] \\ &= \begin{bmatrix} k_1 k_b \left(\dot{\bar{\theta}}_\star^2 - \dot{\theta}^2\right) & -k_b k_2 \dot{\theta} & -k_b k_3 \dot{\theta} \\ 0 & 0 & 0 \\ -k_1 \dot{\theta} & 0 & 0 \end{bmatrix}, \\ h(t,x) &= \mathcal{A}_\Delta(t)\ x, \end{aligned} \tag{37}$$

the function

$$u(t,x) = \int_0^t h(\sigma, x) \mathrm{d}\sigma \tag{38}$$

and it's first partial derivatives with respect to t and x must be continuous and bounded. Assuming initial values are chosen sufficiently small, with Property 1, the matrix function $\mathcal{A}_\Delta(t)$ is bounded on the finite time interval $[0, T]$. This also holds for the integrals, and as a result, with sufficiently small ε, the matrix inversion is possible. Accordingly, continuity follows from continuity of $\mathcal{A}(t)$. This means, that on the interval $[0, T]$, the average system is an $\mathcal{O}(\varepsilon)$ approximation of the closed-loop system (27). This average system is exponentially stable. Thus, with sufficiently small initial conditions:

$$\begin{aligned} ||x_\perp(T)|| &< ||x_\perp(0)|| \\ ||w_1(T) - w_0(T)|| &< ||w_1(0) - w_0(0)||. \end{aligned}$$

Using the latter inequality and Property 1 it follows that $||\dot{\theta}(t) - \dot{\theta}_\star(t)||$ is also bounded on the interval $[T, 2T]$. This also holds for

$$\left|\left| \int_T^{2T} \mathcal{A}_\Delta(\sigma)\ \mathrm{d}\sigma \right|\right|. \tag{39}$$

Following inductive arguments, boundedness holds on $[0, nT],\ n \geq 1$. In fact, due to exponential stability of the average system

$$\exists m \in \mathbb{N} : ||\dot{\theta}(t) - \dot{\theta}_\star(t)|| < ||\dot{\theta}(0) - \dot{\theta}_\star(0)|| \ \forall t > mT.$$

This implies that the approximation by the average system is valid on the infinite interval and gets even better with large time. Hence, the origin is a locally exponentially stable equilibrium of the transverse dynamics and w_1 converges to the orbit exponentially. ■

The advantages of the controller (26) compared to the LQR-based controller are obvious. For LQR-design, the periodic Riccati differential equation needs to be solved, which requires tremendous computational and implementational effort (see e.g. [14]). However, this can be done offline. Result of such a computation is a time-varying control gain matrix, that must somehow be implemented on real-time control hardware. This is typically done either by memory-intensive look-up tables or by computation-intensive interpolation methods. A further challenge when implementing the LQR-based approach is the computation of a projection operator $\mathcal{T}(\theta, \dot{\theta})$ which is able to recover the time (in the sense of a measure of progress) on the limit cycle [10].

In comparison, the controller we propose is parametrized by simply choosing three constants k_1, k_2 and k_3 according to Lemma 1. There is no need to generate a time-varying signal in the controller, which makes implementation almost trivial. Instead of a controller-generated time-varying signal, we use $\dot{\theta}$ as an estimate from an observer in the control law and thereby also bypass computing a projection operator. Indeed, this is a fascinating result: A planned periodic motion[5] is stabilized without the need to generate a periodic signal in the controller.

C. High Gain Observer

The controllers in the previous sections require angular rates of the pendulum angle θ and the reaction wheel angle φ. Since experiments showed that dirty derivative observers did not provide estimates of sufficient quality the approach from [7] was followed and a high-gain observer implemented, see e.g. [13, Chap. 14.5]. To avoid peaking, the angular velocity estimates were saturated at $\dot{\theta}_o = 25\ \mathrm{s}^{-1}$ and $\dot{\varphi}_o = 100\ [\mathrm{s}^{-1}]$. In the implementation of the observer the derivative was approximated with the difference quotient. The observer ran with the same sample time T_s as the controller, see Tab. II. A suitable choice for the parameters of the observer were $\kappa_{i,j} = 1\ \forall i, j$ and $\epsilon = 0.1$.

V. Simulation Results

All applications of the method involving virtual constraints and the transverse dynamics (see [7], [8], [9], [10]) use LQR to stabilize the transverse dynamics. In this section we qualitatively compare such an LQR-based controller to our controller. Benchmark is the linear system with periodic coefficients from (25), with initial value $x_\perp(0) = [1\ 1\ 1]^T$. The weighting matrices of the LQR were chosen to be identity matrices, which is sufficient for qualitative comparison. For LQR design a matrix Riccati differential equation needs to be solved, which was done for the discretized version of (25) using the Matlab script from [15]. Our controller was parametrized with $k_2 = 3$, $k_3 = 3.5$ and $k_1 = 90.3$, which is four times the lower bound from (30). The constants k_2 and k_3 were selected such that the eigenvalues of the filter $x_{\perp,2}, x_{\perp,3}$ are at -1.5 and -2. The parameters of the LTV were chosen according to the model of the RWP and the desired motion

[5] around an unstable equilibrium of an underactuated nonlinear system

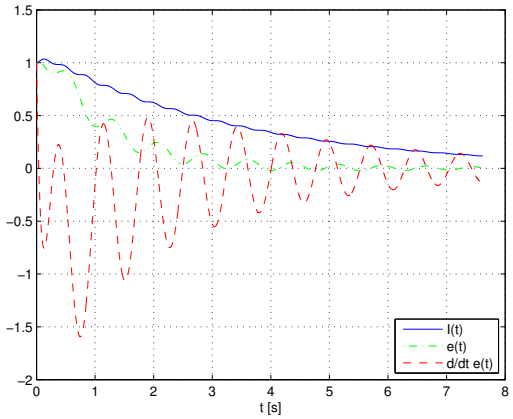

Fig. 2. Evolution of $x_{\perp,1}(t) = I(t)$ (blue, solid), $x_{\perp,2}(t) = e(t)$ (green, dash-dotted) and $x_{\perp,3}(t) = \dot{e}(t)$ (red, dashed) in closed loop with a LQR.

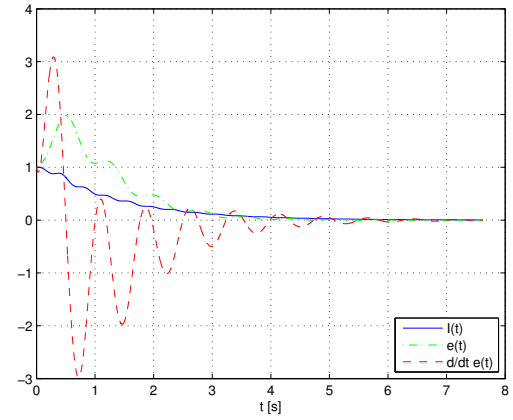

Fig. 3. Evolution of $x_{\perp,1}(t) = I(t)$ (blue, solid), $x_{\perp,2}(t) = e(t)$ (green, dash-dotted) and $x_{\perp,3}(t) = \dot{e}(t)$ (red, dashed) in closed loop with the proposed controller.

$d_1 = -20$, $\theta_\star(0) = 182°$, $\dot{\theta}_\star(0) = 0$. Numerical values for $\theta_\star(t)$ were obtained from simulation of (13). The evolution of $x_\perp(t)$ over $t \in [0, 10 \cdot T]$ under LQR control is shown in Fig. 2, the result of our controller in Fig. 3. When comparing these diagrams recall that the weighting matrices of the LQR were simply chosen as identity matrices, thus additional tuning could possibly lead to faster convergence. The figures should only demonstrate qualitatively that the performance of our controller is comparable to the LQR. Anyway, the ultimate stability criterion for linear systems with periodic coefficients is that the absolute of each eigenvalue of the monodromy matrix (the characteristic multipliers) must be lower than unity [16]. This criterion can be evaluated numerically and gives $\mu_1 = [0.0000 \;\; 0.3855 + 0.3070j \;\; 0.3855 - 0.3070j]^T$ for our controller and $\mu_2 = [0.0005 \;\; 0.7993 \;\; 0.4652]^T$ for the LQR. Also the control input ν shows qualitatively comparable values, see Fig. 4. However, note that ν does not correspond to a physical input of the RWP but is the input to the partial feedback linearization from (22).

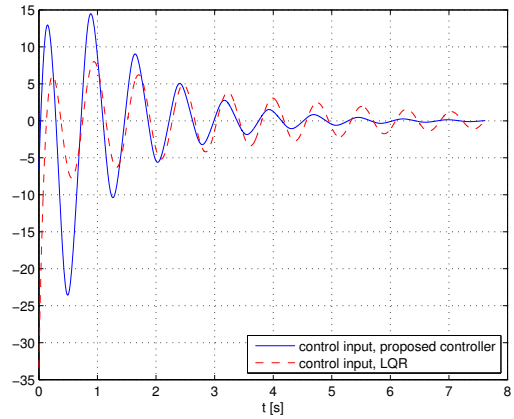

Fig. 4. Evolution of the control input $\nu(t)$ (blue, solid) of our controller, and (red, dashed) of the LQR.

TABLE II
PERIODIC MOTION CONTROLLER PARAMETERS

Symbol	Value [Unit]	Meaning
d_1	-20	virtual constraint parameter
$\theta_\star(0)$	187 [°]	target limit cycle initial angle
$\dot{\theta}_\star(0)$	0 [s^{-1}]	target limit cycle initial rate
k_1	225.8	controller gain 1
k_2	3	controller gain 2
k_3	3.5	controller gain 3
T_s	0.001 [s]	sample time

VI. EXPERIMENTAL RESULTS

Experiments were carried out with different motion parametrizations d_1, $\theta_\star(0)$, $\dot{\theta}_\star(0)$ and different controller gains k_1, k_2, k_3. It must be mentioned that the choice of $\theta_\star(0)$ is the most critical one: For $\theta_\star(0)$ too big, actuator bounds will prevent the controller from stabilizing the limit cycle. On the other hand, choosing $\theta_\star(0)$ too small makes friction the dominant factor and generates unsatisfying results.

The results presented here are for the same parameter values as in the previous section and are summarized in Tab. II. For the first experiment, the pendulum was brought to a state close to the upper equilibrium by lifting it up by hand. Then, the periodic motion controller was switched on. The upper diagram in Fig. 5 shows the resulting motion of the pendulum $(\theta(t), \dot{\theta}(t))$ over time. The lower diagram presents the corresponding phase-plot, where the red curve is the target limit cycle. The small black circle marks the initial state. The figure confirms the ability of the controller to drive the reaction wheel pendulum towards the desired limit cycle. A slight deviation from simulation results is the small buckle in the lower right part of the phase plot. We believe that this is a result of model simplification, most likely caused by gear box back lash since this buckle always occurs immediately after the velocity changes its sign. After the system has reached the limit cycle we have introduced a distortion by touching the pendulum bar. Results are shown in Fig. 6. Although the distortion amounts about half the amplitude, the controller is

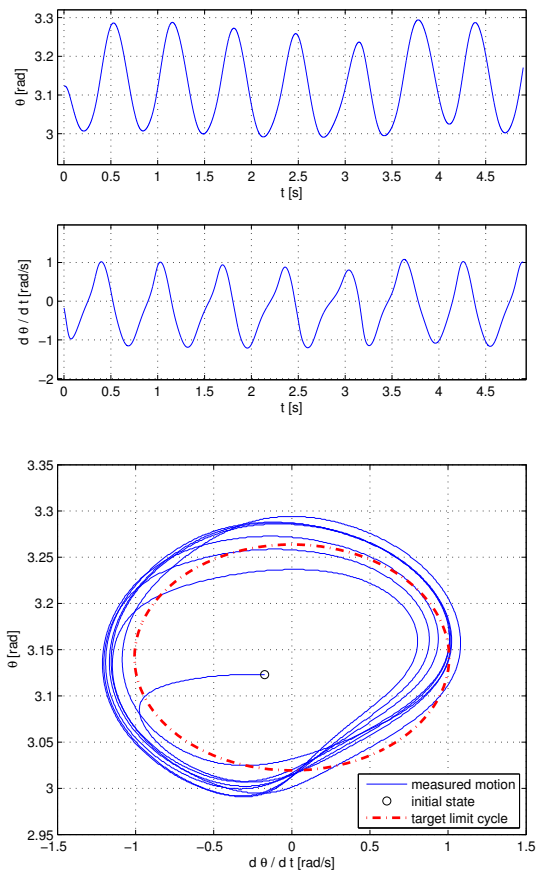

Fig. 5. Resulting motion of the pendulum $(\theta(t), \dot{\theta}(t))$ over time (above) and the corresponding phase-plot (below), where the red dash-dotted curve is the target limit cycle.

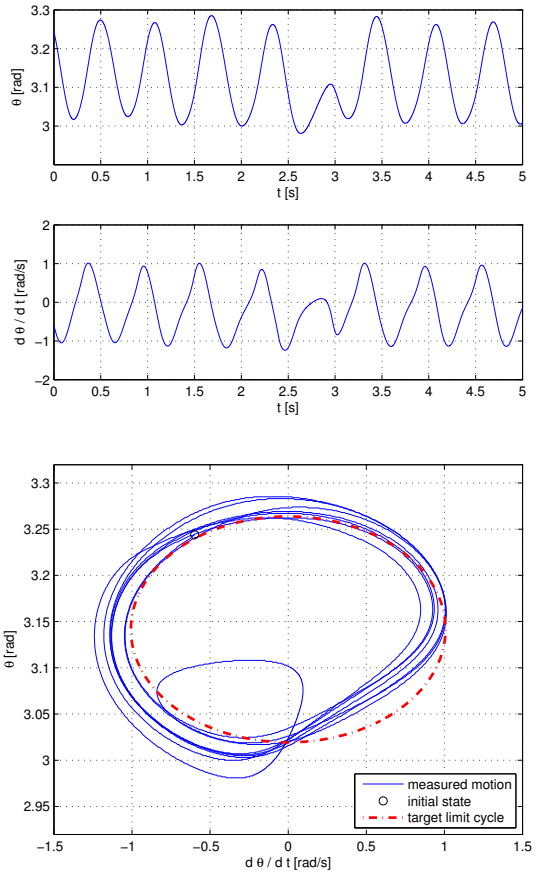

Fig. 6. Limit cycle motion of the pendulum distorted by a short touch of the pendulum bar at ~ 2.5 [s].

able to reestablish the target motion.

VII. Conclusion

In this paper, we successfully designed and implemented a controller for stabilizing periodic motions for an underactuated nonlinear system with unstable equilibria, demonstrated on the reaction wheel pendulum. We applied a modern method from model based nonlinear control which is based on virtual holonomic constraints [7], [8], [9], [10]. The proposed method consists of three steps: 1) motion planning 2) partial feedback linearization and 3) designing a controller for a linear system with periodic coefficients. Earlier applications solved step 3 using LQR, resulting in a time-varying control gain matrix function, which requires fairly large computational effort in design and implementation. Our main contribution is the application of a different method to solve step 3 which is analytic and bases upon perturbation analysis. We are thereby able to radically reduce control design and implementation effort. The proposed controller was compared to the LQR in simulations. Furthermore, the overall method was validated by experiments in a real-world setting. Although modeling was done with ideal assumptions such as no friction, the controller showed sufficient robustness to deal with external disturbances.

Acknowledgment

The authors would like to thank Friedrich Hanser for his astute comments.

References

[1] K. J. Åström, D. J. Block, and M. W. Spong, *The Reaction Wheel Pendulum*. Morgan & Claypool, 2007.

[2] M. Spong and P. Corke, "Nonlinear control of the reaction wheel pendulum," *Automatica*, 2001.

[3] S. Ramamoorthy and B. Kuipers, "Qualitative heterogeneous control of higher order systems," *Hybrid Systems: Computation and Control*, pp. 417–434, 2003.

[4] R. Ortega, M. Spong, F. Gómez-Estern, and G. Blankenstein, "Stabilization of a class of underactuated mechanical systems via interconnection and damping assignment," *IEEE Transactions on Automatic Control*, vol. 47, no. 8, pp. 1218–1233, 2002.

[5] V. Santibanez, R. Kelly, and J. Sandoval, "Control of the inertia wheel pendulum by bounded torques," in *CDC-ECC'05 - European Control Conference and 44th IEEE Conference on Decision and Control 2005*, vol. 1, no. 3. IEEE, 2005, pp. 8266–8270.

[6] L. T. Aguilar, I. Boiko, L. Fridman, and L. Freidovich, "Inducing oscillations in an inertia wheel pendulum via two-relays controller: Theory and experiments," *American Control Conference 2009*, pp. 65–70, 2009.

[7] L. B. Freidovich, P. X. La Hera, U. Mettin, A. Robertsson, A. S. Shiriaev, and R. Johansson, "Shaping Stable Periodic Motions of Inertia Wheel Pendulum: Theory and Experiment," *Asian Journal of Control*, vol. 11, no. 5, 2009.

[8] A. S. Shiriaev, J. W. Perram, and C. Canudas-de Wit, "Constructive tool for orbital stabilization of underactuated nonlinear systems: virtual constraints approach," *IEEE Transaction on Automatic Control*, vol. 50, pp. 1164–1176, 2005.

[9] A. Shiriaev, J. Perram, A. Robertsson, and A. Sandberg, "Periodic motion planning for virtually constrained Euler-Lagrange systems," *Systems and Control Letters*, vol. 55, pp. 900–907, 2006.

[10] A. S. Shiriaev, L. B. Freidovich, and I. R. Manchester, "Can we make a robot ballerina perform a pirouette? Orbital stabilization of periodic motions of underactuated mechanical systems," *Annual Reviews in Control*, vol. 32, no. 2, pp. 200–211, 2008.

[11] S. M. LaValle, *Planning Algorithms*. Cambridge: Cambridge University Press, 2006.

[12] C. Chevallereau, G. Abba, Y. Aoustin, F. Plestan, E. Westervelt, C. Canudas-de Wit, and J. Grizzle, "RABBIT: A testbed for advanced control theory," *IEEE Control Systems Magazine*, vol. 23, no. 5, pp. 57–79, Oct. 2003.

[13] H. K. Khalil, *Nonlinear Systems*, 3rd ed. Prentice-Hall, 2002.

[14] S. Gusev, S. Johansson, B. Kågström, A. Shiriaev, and A. Varga, "A numerical evaluation of solvers for the periodic Riccati differential equation," *BIT Numerical Mathematics*, vol. 50, no. 2, pp. 301–329, 2010.

[15] I. Houtzager, "DPRE - Discrete-time periodic Riccati equation solver for periodic LQ state-feedback design," 2008. [Online]. Available: http://www.mathworks.co.kr/matlabcentral/fileexchange/21379-dpre

[16] W. Hahn, *Stability of Motion*. Springer, 1967.